

Size Variability of the Unit Building Block of Peripheral Light-Harvesting Antennas as a Strategy for Effective Functioning of Antennas of Variable Size that Is Controlled *in vivo* by Light Intensity

A. S. Taisova, A. G. Yakovlev, and Z. G. Fetisova*

Belozersky Research Institute of Physico-Chemical Biology, Lomonosov Moscow State University, 119992 Moscow, Russia; fax: (495) 939-3181; E-mail: zfetisova@genebee.msu.ru; zfetisova@belozersky.msu.ru

Received November 14, 2013

Revision received December 2, 2013

Abstract—This work continues a series of studies devoted to discovering principles of organization of natural antennas in photosynthetic microorganisms that generate *in vivo* large and highly effective light-harvesting structures. The largest antenna is observed in green photosynthesizing bacteria, which are able to grow over a wide range of light intensities and adapt to low intensities by increasing of size of peripheral BChl *c/d/e* antenna. However, increasing antenna size must inevitably cause structural changes needed to maintain high efficiency of its functioning. Our model calculations have demonstrated that aggregation of the light-harvesting antenna pigments represents one of the universal structural factors that optimize functioning of any antenna and manage antenna efficiency. If the degree of aggregation of antenna pigments is a variable parameter, then efficiency of the antenna increases with increasing size of a single aggregate of the antenna. This means that change in degree of pigment aggregation controlled by light-harvesting antenna size is biologically expedient. We showed in our previous work on the oligomeric chlorosomal BChl *c* superantenna of green bacteria of the Chloroflexaceae family that this principle of optimization of variable antenna structure, whose size is controlled by light intensity during growth of bacteria, is actually realized *in vivo*. Studies of this phenomenon are continued in the present work, expanding the number of studied biological materials and investigating optical linear and nonlinear spectra of chlorosomes having different structures. We show for oligomeric chlorosomal superantennas of green bacteria (from two different families, Chloroflexaceae and Oscillochloridaceae) that a single BChl *c* aggregate is of small size, and the degree of BChl *c* aggregation is a variable parameter, which is controlled by the size of the entire BChl *c* superantenna, and the latter, in turn, is controlled by light intensity in the course of cell culture growth.

DOI: 10.1134/S0006297914030110

Key words: photosynthesis, structure and function, peripheral antennas

The structure of the photosynthetic unit (PSU) must be rigidly optimized to function with the high quantum yield ($\phi \geq 90\%$) that is observed experimentally [1]. This means that long-range molecular order must exist in natural PSUs, because only ordered systems may be optimized.

The present work, in accordance with our concept of rigid optimization of the structure of photosynthesizing apparatus on functional criterion [1], continues the tar-

geted search for fundamental principles of organization of natural PSUs that we have theoretically predicted for optimal model light-harvesting systems. This approach produced a set of key principles of organization of PSUs with fixed size [2-9].

The present work continues our investigations of the problem of structural optimization of light-harvesting antennas of variable size, which is controlled *in vivo* by light intensity during growth of microorganisms. Antenna size variability makes the problem of optimization more crucial since the efficiency of energy transfer from the antenna to the reaction centers is inversely proportional to antenna size [1]. Thus, requirements for optimization become stricter upon increasing PSU size.

Abbreviations: ΔA , differential absorption; BChl, bacteriochlorophyll; BPheo, bacteriopheophytin; H, hyperchromism; PSU, photosynthetic unit.

* To whom correspondence should be addressed.

Our previous works have shown that oligomerization (aggregation) of antenna pigments that is provided by specific donor–acceptor properties of chlorophyll is one of universal structural factors that optimize functioning of antenna with any spatial grid [5–9]. These key properties of chlorophylls allow self-aggregation of the pigments [10], and this, in turn, allows self-organization of the order that is crucial for all natural systems.

Earlier, using mathematical modeling of natural PSU functioning, we showed that aggregation of pigments of a model light-harvesting antenna, being itself one of the universal optimizing factors, also allows managing the efficiency of oligomeric antenna (of fixed as well as variable size) functioning by changing the degree of aggregation of light-harvesting pigments [5, 8, 11]. If the degree of aggregation of pigments is a variable factor, then the efficiency of an antenna increases on increasing the single antenna aggregate [5, 11], thereby providing high efficiency of a PSU regardless of its size. Thus, change in the degree of aggregation of pigments that is controlled by size of the light-harvesting antenna is biologically expedient.

It has been shown in our previous work [12] on oligomeric chlorosomal BChl *c* superantenna of green bacteria from the Chloroflexaceae family that the principle of structural optimization of a variable antenna that is controlled by intensity of light in the course of cell culture growth is actually realized *in vivo*.

In the present work we continued studies of this phenomenon and expanded the set of investigated materials and experiments on studying of optical linear and nonlinear spectra of chlorosomes with different structures, isolated from different green bacteria (belonging to Chloroflexaceae and Oscillochloridaceae families [13–15]) adapted to extreme light intensities.

Chlorosomal extramembrane superantennas (chlorosomes) of photosynthesizing green bacteria are of ellipsoidal shape ~70–260 nm in length and ~30–100 nm in width and contain from $\sim 10^4$ to $3 \cdot 10^5$ molecules of the main light-harvesting pigment – bacteriochlorophyll (BChl) *c/d/e* (depending on bacterial species) in an aggregated state. In addition to BChl *c/d/e*, chlorosomes contain carotenoids, quinones, and BChl *a*, which is localized in the base plate (3–4 nm in thickness) connecting the chlorosomes with the cytoplasmic membrane, where the basic BChl *a* antenna and reaction centers are localized [14, 16, 17].

Several models of the three-dimensional structures of chlorosomes of different green bacteria have been published. The diversity of models can be characterized by two types: (i) tubular models, in which BChl *c/d/e* forms hollow rods [18, 19], and (ii) lamellar models, in which BChl *c/d/e* forms parallel planes (lamellas) [20]. Strong orientation ordering of BChl *c* Q_y transition dipoles that has been demonstrated *in situ* [4] as well in isolated antenna complexes [3, 16, 17] means that the elementary struc-

tural element of this superantenna is a (quasi)linear chain of BChl *c/d/e* aggregate. So, all the diversity of models describing the same type of chlorosomes is found in the difference (i) of the number of BChl *c/d/e* chains in each rod, (ii) of the length of these chains (i.e. number of BChl *c/d/e* chains along a rod), (iii) of the structure of these BChl *c/d/e* chains, (iv) of the mode of BChl *c/d/e* chains folding in a rod, and/or (v) of the mode of BChl *c/d/e* chains folding in lamella [21].

The theory we have developed for oligomeric pigment spectroscopy, using electron microscopy data [18, 19], suggests a tubular model of optimal molecular organization of chlorosomal antenna in green bacteria from the Chloroflexaceae family that is consistent with all available spectral data [22–26]. In this model of the chlorosome, each rod of ~100-nm length consists of short elementary rods, each of which contains an elementary building block of oligomeric BChl *c* antenna in the form of a cylindrical aggregate made of six parallel linear chains of BChl *c* oligomers. Neighboring aggregates that belong to the same rod interact with each other weakly because they are at the distance of 20–30 nm. Intermolecular distances in the aggregate provide strong excitonic interaction inside each linear chain ($300\text{--}700\text{ cm}^{-1}$) and weak interaction between neighboring chains (about 50 cm^{-1}) [22–26].

In the present work, we have investigated structural changes in chlorosomal antennas of green bacteria of the Chloroflexaceae and Oscillochloridaceae families that take place during their adaptation to extreme light intensities.

MATERIALS AND METHODS

Microorganisms and cell culture growth conditions.

Photosynthesizing bacteria of two families of green anoxygenic phototrophic filamentous bacteria, Chloroflexaceae and Oscillochloridaceae, were selected as subjects for investigation: the thermophilic bacterium *Chloroflexus (Cfx) aurantiacus*, strain Ok-70-fl (collection of Leiden University, The Netherlands) and the mesophilic bacterium *Oscillochloris (Osc) trichoides*, strain DG-6, a typical strain of *Osc. trichoides* (All-Russian Collection of Industrial Microorganisms, B-10173).

Cultures of the green filamentous thermophilic bacterium *Cfx. aurantiacus* Ok-70-fl were grown under anaerobic conditions at 55°C on standard medium [27] under constant stirring and light intensity of 50 and 1000 W/m².

Cultures of *Osc. trichoides* strain DG-6 were grown under anaerobic conditions in 500 ml flasks at 30°C on modified DGN medium under constant stirring and light intensity of 50 and 1000 W/m² [14, 28].

Isolation of chlorosomes from *Cfx. aurantiacus* and *Osc. trichoides* cells. Chlorosomes were isolated by two

consecutive continuous sucrose concentration gradients (55-20 and 45-15%) in the presence of 10 mM sodium ascorbate and 2 M sodium thiocyanate as described earlier [14, 28].

Absorption spectra were recorded at room temperature on a Hitachi-557 spectrophotometer (Hitachi, Japan). Errors in the spectra did not exceed 3%.

Fluorescence excitation spectra of BChl *a* were recorded at room temperature (295 K) using a Hitachi-850 spectrofluorimeter at emission wavelength of 825 nm. Samples were suspended in 50 mM Tris-HCl buffer (pH 8.0). The absorption of samples was 0.2 optical density units at 750 and 740 nm for *Osc. trichoides* and *Cfx. aurantiacus* chlorosomes, correspondingly. To create strong reductive conditions, chlorosomes were preliminarily incubated for 60 min at 4°C with freshly prepared 20 mM sodium dithionite solution (in 50 mM Tris-HCl buffer, pH 8.0).

Pigment content in samples was determined according to the method of Feick et al. [29]. Samples were treated with 25-fold volume of acetone-methanol mixture (7 : 2 v/v) for 20 min in the dark at 4°C. The absorption of transparent supernatants was measured at the long-wavelength maximums at 769 nm for BChl *a* and 661 nm for BChl *c* using the Hitachi-557 spectrophotometer. Calculations were based on molar extinction coefficients (ϵ) of 68.6 and 74 mM⁻¹·cm⁻¹ for BChl *a* and BChl *c*, respectively, in the acetone-methanol mixture.

Differential absorption spectroscopy with femtosecond resolution. Femtosecond difference absorption (ΔA) spectra were measured with a laser instrument that was developed in the Belozersky Research Institute of Physico-Chemical Biology, Lomonosov Moscow State University. The instrument consists of a mode-locked titanium-sapphire laser, titanium-sapphire multipass amplifier, pulse stretcher-compressor device, single pulse isolation device, continuum generator, pump-probe measuring circuit, and multichannel optical spectrum analyzer (Oriel, France) [12]. Excitation was with 110-fs pulses passed through an interference filter isolating a 10-nm-wide band with absorption maximum 750 nm (i.e. within the BChl *c* Q_y transition region). Femtosecond continuum pulses were used for probing. The probe-excitation pulse time delay varied in 10-fs steps. The excitation/probing pulse energy ratio was 100 : 1. The angle between excitation and probing polarization vectors was 54.7° (the magic angle). Measurements were taken with 15-Hz frequency. The resulting ΔA spectra obtained with averaging over 5000-50,000 spectra for each time delay consisted of 500-1000 points. The sample optical density was 0.5-1.0 (1-mm cuvette). Typical ΔA^{\max} values were 10⁻⁵-10⁻⁴ optical density units measured with 2-10% precision.

The approximate energy density was estimated at 10¹² photons/cm² per pulse. Measurements were taken at room temperature.

RESULTS AND DISCUSSION

All experiments were performed with chlorosome samples isolated from cells of two strains of photosynthesizing bacteria that represent two families of green anoxygenic phototrophic filamentous bacteria, Chloroflexaceae and Oscillochloridaceae: 1) the thermophilic bacterium *Cfx. aurantiacus*, strain Ok-70-fl; 2) the mesophilic bacterium *Osc. trichoides*, strain DG-6.

Cell cultures of these strains were grown under low and high light intensities (differing 20-fold) that in cell cultures of both strains lead to different molar ratio of chlorosomal BChl *c* (B740/B750 nm) to membranous BChl *a* (B866/B860 nm). At the same time, the ratio of the number of membranous BChl *a* (B866/B860 nm) molecules per reaction center in antennas, located near the center, does not depend on the light intensity in the course of cell culture growth. So, using our suggested definition [12], we identified both *Cfx. aurantiacus* cultures by parameter η that characterizes the ratio of absorption maximums of chlorosomal BChl *c* (B740 nm) and membranous BChl *a* (B866 nm): $\eta = 8$ and 32. We designated chlorosome samples isolated from these cultures as C-8 and C-32, correspondingly, that indicates their origin from cultures having the corresponding parameters $\eta = 8$ and 32. Thus, the size of BChl *c* antenna in the second culture ($\eta = 32$) is approximately four times greater than those in the first culture ($\eta = 8$). Absorption spectra of cells and chlorosomes isolated from these cells of two cell cultures of *Cfx. aurantiacus* with different content of BChl *c* that determines the size the *Cfx. aurantiacus* PSU are shown in Fig. 1. Excitation energy transfer efficiency from B740 to B795 (the terminal acceptor subantenna of a chlorosome) was estimated by the standard method as 80% in both chlorosome samples at room temperature (20°C) [26]. At ambient temperatures (50-60°C), *Cfx. aurantiacus* chlorosomes have an efficiency of BChl *c*→BChl *a* energy transfer close to 100% [30].

The amplitude of the absorption peak of BChl *a* (860 nm) is extremely small in the absorption spectra of *Osc. trichoides* cells, so chlorosomes samples isolated from *Osc. trichoides* cultures cultivated at low (50 W/m²) and high (1000 W/m²) light intensities were identified in accordance with BChl *c*/BChl *a* molar ratio, which was determined using absorption spectra of chlorosomes in acetone-methanol [29]. Samples of isolated chlorosomes were designated as C-70 and C-110 in accordance with the determined molar BChl *c* : BChl *a* ratios, which are 70 : 1 (1000 W/m²) and 110 : 1 (50 W/m²), correspondingly. Absorption spectra of chlorosomes isolated from *Osc. trichoides* cultures with different BChl *c* content are shown in Fig. 2.

According to our model of BChl *c* organization in chlorosomes of *Cfx. aurantiacus* [26], the elementary building block of chlorosomal BChl *c* antenna has the shape of a cylindrical aggregate that is formed by exciton-

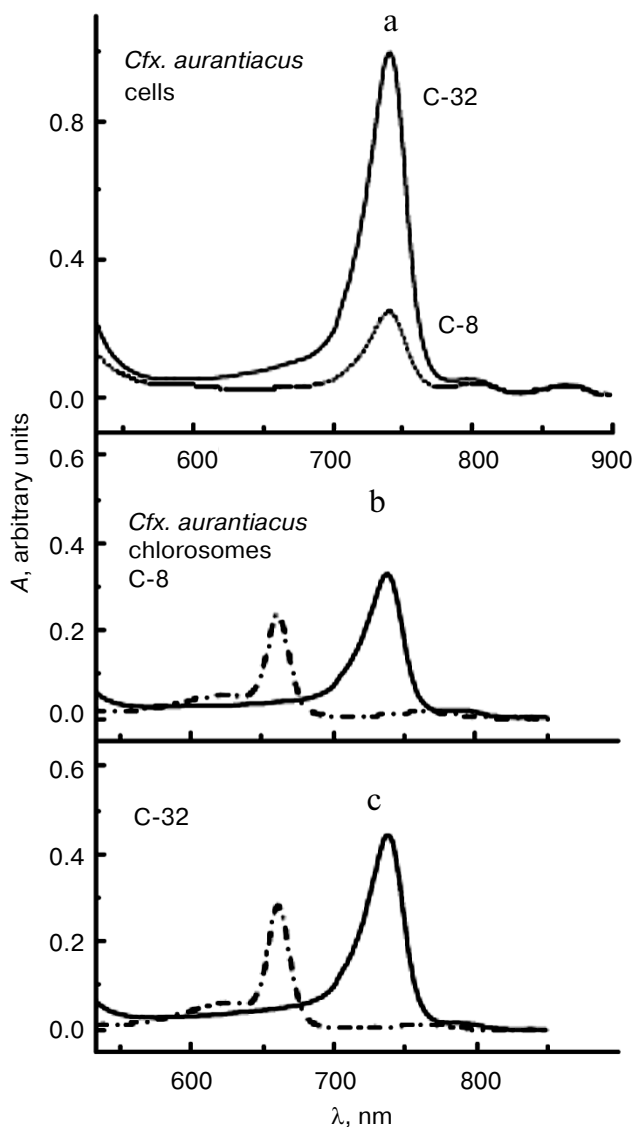


Fig. 1. Absorption spectra of cells (a) and chlorosomes (b, c) isolated from *Cfx. aurantiacus* cultures with different parameter η ($\eta = 8$ and 32). a) Cells (in 50 mM Tris-buffer, pH 8.0) from cultures with parameter $\eta = 32$ (solid line) and parameter $\eta = 8$ (dotted line). The absorption maximum at 740 nm belongs to chlorosomal BChl *c*; the absorption maximums at 808 and 866 nm belong to membranous antenna BChl *a*. The spectra were normalized at absorption maximum of core BChl *a* antenna (866 nm). b, c) Chlorosomes in 50 mM Tris-buffer (pH 8.0) (solid lines) and in acetone–methanol (7 : 2) (dash-dotted lines). The absorption maximum at 740 nm belongs to chlorosomal BChl *c*; the absorption maximum at 795 nm belongs to chlorosomal BChl *a*. Cells and chlorosomes are designated by indexes C-8 and C-32 according to their origin from cultures having parameters $\eta = 8$ and 32, correspondingly. Parameter η , which is equal to the ratio of amplitudes of long-wave absorption maxima of chlorosomal BChl *c* (740 nm) and membranous BChl *a* (866 nm), characterizes BChl *c* content in chlorosomes of two different cultures: $\eta = A_{740}/A_{866} = 8$ and 32.

ically coupled linear chains of BChl *c* oligomers. The amplitude of the BChl *c* band bleaching in differential absorption spectra of chlorosomes at zero time delay must be increased with increasing oligomer length [31] because

the formation of linear oligomers containing n monomers leads to more than n times increase in dipole strength of the Q_y band of BChl *c* absorption spectra in comparison with its monomeric form [22]. This effect is only expected in the limits of small size of an oligomer: $n < n_C$, where n_C is the critical size of an oligomer (aggregate) [31], because only in this case delocalization of excitation practically coincides with physical size of the aggregate. Estimation of this value for photosynthetic pigments gives $n_C \approx 5$ [32]. Because the length of the linear chain of BChl *c* oligomers forming elementary cylindrical BChl *c* aggregates does not exceed the value $n = 6$ in the frames of our model of aggregation of chlorosomal pigments [25], then the nonlinear optical spectroscopy that is sensitive to the size of aggregate [31, 32] is the most informative experimental method for the determination. Thus, investigation of dependence of amplitude of BChl *c* band bleaching in differential absorption spectra of chlorosomes with different content of BChl *c* (i.e. chlorosomes of different size) at zero time delay is the decisive experiment for registration of changes in the degree of pigment aggregation, which was also demonstrated in previous works [12].

Figure 3 shows isotropic ΔA spectra of chlorosome samples, C-8 and C-32, isolated from *Cfx. aurantiacus* cultures adapted to two extreme light intensities (low and high) that caused four-fold change in BChl *c* concentration in the samples.

The ΔA spectra of these chlorosomes were measured at room temperature in the spectral region 710–830 nm with various time delays: 1) with delay of 200 fs corresponding to maximal ΔA amplitude of BChl *c* for both samples in wavelength region about 750 nm, and 2) time delays of 25 and 100 ps corresponding to maximal ΔA amplitude of BChl *a* at 795 nm for chlorosomes C-8 and C-32, correspondingly. In all the experiments effects of multiphoton processes were insignificant because the exciting intensities used here correspond to the linear region of amplitude changes in the case of BChl *c* as well as BChl *a*, and the shape of the ΔA spectra did not change in the limits of this linear region [25, 26].

The ΔA spectra shown in Fig. 3 are presented so as to give maximal amplitudes of ΔA spectra of BChl *a* for all samples equal. The main features of each spectrum presented in Fig. 3 are similar to those measured by us earlier for *Cfx. aurantiacus* chlorosomes [12]. At delay of 200 fs, each ΔA spectrum demonstrates BChl *c* maximum at 750 nm corresponding to the superposition of bleaching and stimulated emission bands and is followed by BChl *c* maximum at 730 nm associated with BChl *c* absorption from the excited state. When excitation energy transfer from BChl *c* to BChl *a* is practically completed (i.e. after 25 and 100 ps for C-8 and C-32 samples, correspondingly), the ΔA spectra for BChl *a* are observed demonstrating only one bleaching/stimulated emission band with maximum at 795 nm, reproducing the shape of absorption spectra for chlorosomal BChl *a* antenna B795. Normal-

ized spectra of the two chlorosome samples with different size clearly demonstrate the identity of the ΔA spectra for BChl *a* measured in the 770–830 nm region (Fig. 3). This means that the BChl *a* subantenna pigments function as monomers independently on the size of the chlorosomes (see also [26]). A similar conclusion was first made for *Cfx. aurantiacus* BChl *a* subantenna in our work [33].

Comparison of ΔA spectra measured near zero time delay in the 710–830 nm range shows that increase in BChl *c* content in chlorosomes is accompanied by ΔA spectra for BChl *c* that demonstrate (i) *red shift* (by 6.1 nm), (ii) *narrowing of bands* (by 2.9 nm), and (iii) *increase in amplitudes* (up to 2.2-fold).

Comparison of the analogous ΔA spectra near zero time delay in the 710–830 nm range measured in the present work (for two samples, C-8 and C-32, with four-fold change in the chlorosomal antenna size) with those meas-

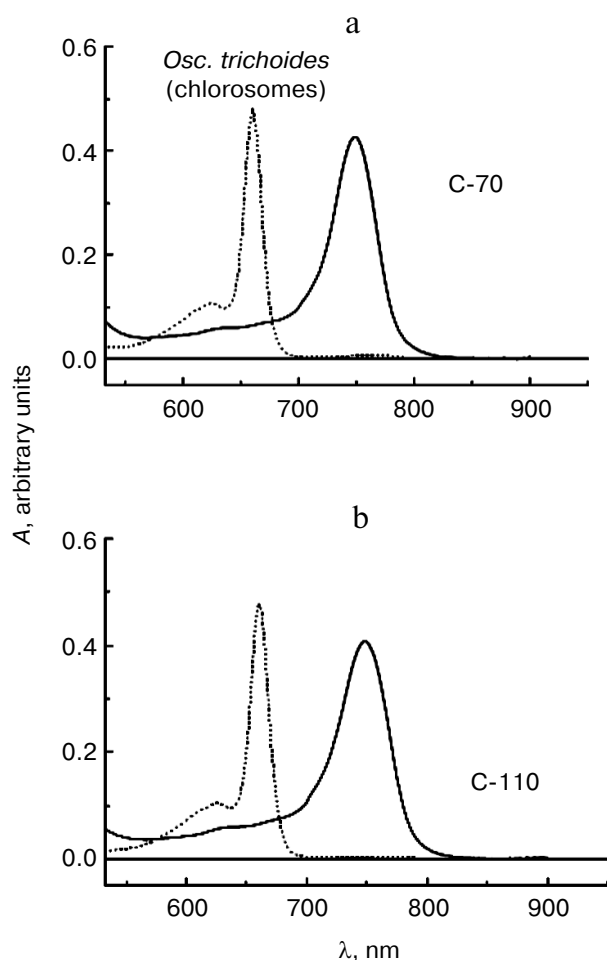


Fig. 2. Absorption spectra of chlorosomes isolated from *Osc. trichoides* cell cultures in 50 mM Tris-buffer (pH 8.0) (solid lines) and their pigments in acetone–methanol (7 : 2) (dotted lines). Cultures grown under light of 1000 W/m² (BChl *c* : BChl *a* molar ratio equal to 70 : 1) are designated as C-70. Cultures grown at light of 50 W/m² (BChl *c* : BChl *a* molar ratio is 110 : 1) are designated as C-110.

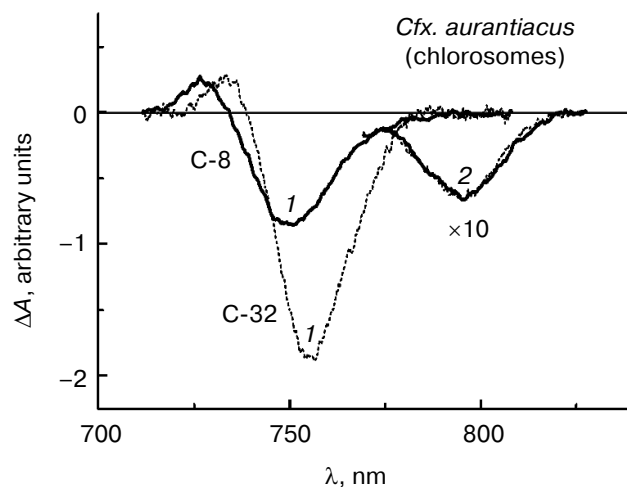


Fig. 3. Isotropic ΔA spectra measured at room temperature for two chlorosome samples of *Cfx. aurantiacus*, C-8 (solid lines) and C-32 (dotted lines), with different time delays: 1) with time delay of 200 fs corresponding to the maximal ΔA amplitude of BChl *c* for both chlorosomes samples in the wavelength region about 750 nm, and 2) with time delays of 25 and 100 ps that correspond to maximal ΔA amplitude of BChl *a* at 795 nm for chlorosomes C-8 and C-32, respectively. Excitation wavelength, 750 nm; duration of exciting impulse, 110 fs. The ΔA spectra were normalized to provide equal amplitudes of BChl *a* ΔA spectra for all the chlorosome samples. The ΔA amplitudes of BChl *a* spectra with maximum at 795 nm measured with picosecond delays were multiplied by 10.

ured earlier for *Cfx. aurantiacus* chlorosomes with intermediate size antennas (for four samples, C-10, C-16, C-24, and C-30 [12]) clearly demonstrates that *sequential* increase in BChl *c* content in six samples of chlorosomes of different size is accompanied by ΔA spectra for BChl *c* that demonstrate (i) *sequential red shift*, (ii) *sequential narrowing of bands*, and (iii) *sequential increase in amplitudes* of these spectra (Table 1).

All of the principal changes in BChl *c* ΔA spectra (measured near zero time delay (Fig. 3 and Table 1)) accompanying increase in BChl *c* in chlorosomes, i.e. *sequential increase in amplitude*, *red shift*, and *bleaching band narrowing*, are predicted by a theory of nonlinear optical spectroscopy for (quasi)linear aggregates that increase in size and are confirmed experimentally in the present work and in a number of other studies [12, 25, 26, 31, 32, 34–37]. In particular, the main changes in the initial ΔA spectra for BChl *c* as the length of linear chain of BChl *c* oligomers forming elementary cylindrical BChl *c* aggregate increased have been shown in theoretical calculations for our model of *Cfx. aurantiacus* chlorosome (if other parameters of the unit aggregate structure are unchanged) [25, 26]. However, such spectral changes can be observed only in the limits of a small aggregate. It is necessary to note that the shape of differential absorption spectra for a cylindrical aggregate formed by linear chains of BChl *c* oligomers with weak interaction between neighboring chains [22, 25, 26] is mainly determined by inter-

Table 1. Parameters of BChl *c*-bleaching band in ΔA spectra measured for six chlorosome samples of *Cfx. aurantiacus* with time delay of 200 fs

C- η	$-\Delta A^{\max}$, relative units	λ (ΔA^{\max}), nm	FWHM, nm
C-8	1.00	749.9	22.7
C-10	1.14	750.8	22.1
C-16	1.58	753.4	21.4
C-24	1.88	754.7	20.5
C-30	2.18	755.5	20.1
C-32	2.21	756.0	19.8

Note: For each chlorosome sample the following data are given: 1) maximal amplitude of bleaching band ($-\Delta A^{\max}$) normalized to amplitude ($-\Delta A^{\max}$) for chlorosomes C-8; 2) position of band maximum (λ (ΔA^{\max})), and 3) full width at half maximum (FWHM). To demonstrate the trends in the experimental spectra parameters, data for chlorosomes C-8 and C-32 were supplemented with the data for chlorosomes C-10 through C-30 that were obtained from spectra presented in our previous publication [12].

actions inside the chain [25]. As a result, the dependence of shape and amplitude of differential absorption on the length (n) of BChl *c* oligomer (where n is the number of monomers in the elementary cylindrical aggregate chain) [12, 25, 26] is analogous to such dependencies for a (quasi)linear aggregate of variable size [31, 32, 36]. Thus, in the case of the studied BChl *c* oligomers, $n < 6$ [12, 25, 26], i.e. n corresponds to the limit of bacterial antenna small aggregate ($n_c \approx 5$ [23]), when the bleaching amplitude increases proportionally to n [12, 25, 26, 31, 32]. Under this limit, the coherence (delocalization) length that is probed by nonlinear absorption differential spectra differed insignificantly from the physical size n of the aggregate. Thus, the observed difference in initial ΔA spectra for *Cfx. aurantiacus* BChl *c* in chlorosomes of different size demonstrates increase in the size of the unit building block of BChl *c* antenna (i.e. increase in the unit BChl *c* oligomer length) when the entire BChl *c* antenna is increased.

It is necessary to note that in the limits of a large aggregate ($n \gg 5$), the bleaching amplitude in case of increasing n increases more slowly (if it increases), and spectral shift and bleaching band narrowing is practically not observed [31, 32]. In these limits, the length of coherency can be sufficiently lower than the physical size n of the aggregate [32, 34]. This limit is characteristic for BChl *a* aggregates of LH1-/LH2 antennas of purple bacteria [31, 32, 34-36], and also for B866 aggregate of membranous BChl *a* antenna of the green bacterium *Cfx. aurantiacus* [37].

For the entire series of *Cfx. aurantiacus* chlorosomes (from C-8 to C-32 samples), the BChl *c* ΔA spectra meas-

ured near zero time delay increased by 2.2-fold when the chlorosomal antenna size increased approximately 4-fold. This means (see above) that in studied chlorosomes the size of the unit building block of BChl *c* antenna approximately increased 2-fold when the size of the entire BChl *c* antenna increased 4-fold, i.e. under increase in *Cfx. aurantiacus* PSU size.

The BChl *c*/BChl *a* molar ratio in *Osc. trichoides* chlorosomes is significantly higher than that in *Cfx. aurantiacus* chlorosomes (not less than four times greater in natural conditions) [14, 38]. So, it is impossible to register ΔA spectra of BChl *a* in *Osc. trichoides* chlorosomes in contrast to *Cfx. aurantiacus* chlorosomes.

However, a conclusion regarding the size and size variability of elementary BChl *c* oligomer *in vivo* can be obtained in independent experiment studying the antenna size dependent hyperchromism of the Q_y absorption band of the chlorosomal oligomeric BChl *c* antenna. This specific question has been addressed in the present experiment.

Formation of BChl oligomers leads to a substantial increase in the oscillator strength of the Q_y absorption band (in comparison to monomeric pigments) at the expense of the B_y band. It was predicted for BChl/BPheo *a* [21] that this effect increases with an increase in oligomer length under certain limitations concerning the length.

The hyperchromism (H) of the BChl *c* Q_y absorption band in each chlorosome sample was determined from the ratio of oscillator strength of oligomeric BChl *c* Q_y band *in vivo* (absorption bands with maxima at 740 and 750 nm for *Cfx. aurantiacus* (Fig. 1) and *Osc. trichoides* (Fig. 2) chlorosomes) to the oscillator strength of monomeric BChl *c* Q_y band *in vitro* (absorption bands with maxima at 660 nm for extracts of chlorosomes of *Cfx. aurantiacus* (Fig. 1) and *Osc. trichoides* (Fig. 2) in acetone-methanol with the same concentration of BChl *c* as

Table 2. Relative value of hyperchromism (H) of absorption Q_y band for BChl *c* of *Cfx. aurantiacus* chlorosomes, C-8 through C-32

<i>Cfx. aurantiacus</i> chlorosomes	H, relative units
C-8	1.00
C-10	1.01
C-16	1.11
C-24	1.23
C-30	1.31
C-32	1.33

Note: The chlorosome C-8 hyperchromism value was taken as 1.0.

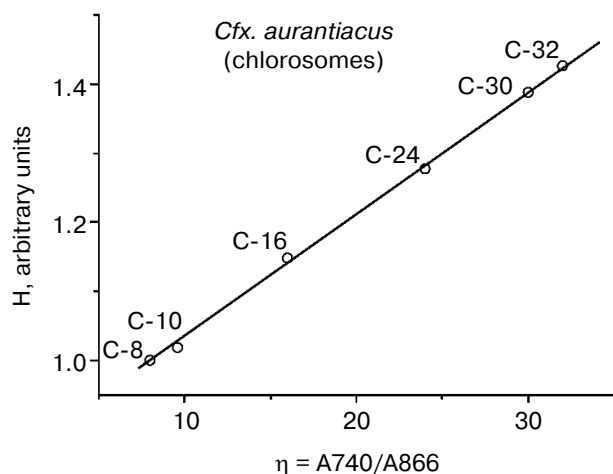


Fig. 4. Relative value of hyperchromism (H) of chlorosomal BChl *c* absorption Q_y band calculated for six samples of *Cfx. aurantiacus* chlorosomes, C-8, C-10, C-16, C-24, C-30, and C-32. All calculated H values were normalized to the hyperchromism value for chlorosomes C-8.

in vivo). The BChl *c* Q_y band hyperchromism was calculated by averaging the data obtained during measurements of 10 chlorosome spectra *in vivo* and 10 chlorosome spectra *in vitro*.

It has been shown that hyperchromism of the BChl *c* Q_y band increases with increase in BChl *c* antenna size that is under control of light intensity during cell growth [39], and this effect is reliably observed for both *Cfx. aurantiacus* and *Osc. trichoides* chlorosomes.

To compare experimental and calculated [39-41] data and exclude unknown parameters, we used normalized H values, i.e. all H values obtained for *Cfx. aurantiacus* chlorosomes were normalized against minimal H value measured for chlorosomes with minimal BChl *c* antenna, i.e. for C-8. In case of *Osc. trichoides* chlorosomes, the experimental H values were normalized against the minimal H value that was obtained for chlorosomes with minimal BChl *c* antenna, i.e. for C-70.

Table 2 contains results of hyperchromism calculations for the series of investigated samples of *Cfx. aurantiacus* chlorosomes, C-8, C-10, C-16, C-24, C-30, and C-32 with four-fold changing of chlorosomal antenna size from C-8 to C-32 (i.e. from $\eta = 8$ to $\eta = 32$). Figure 4 shows the dependence of the relative value of chlorosomal BChl *c* absorption Q_y band hyperchromism on the *Cfx. aurantiacus* chlorosome antenna size, $H(\eta)$, for the six samples of *Cfx. aurantiacus* chlorosomes, C-8, C-10, C-16, C-24, C-30, and C-32.

Figure 4 clearly demonstrates that (i) *sequential* four-fold increase in chlorosomal BChl *c* antenna is accompanied by *sequential* increase by 33% in hyperchromism of oligomeric BChl *c* absorption Q_y band and (ii) this dependency is strictly linear.

Both experimental facts were predicted by the theory of absorption Q_y band hyperchromism developed for BChl *c* oligomers [39-41] and give two key conclusions:

- the size of the unit BChl *c* oligomer (*n*) in *Cfx. aurantiacus* chlorosomes corresponds to the limit of the small aggregate size of bacterial antenna of *Cfx. aurantiacus* ($n \approx 5$);
- increase in entire chlorosomal antenna in *Cfx. aurantiacus* causes increase in its unit BChl *c* oligomer size.

Hyperchromism ceases to increase in BChl *c* oligomers with $n > 10$ [40, 41].

Results of calculations of hyperchromism relative values of BChl *c* absorption Q_y band of *Osc. trichoides* chlorosomes C-70 and C-110 are presented in Table 3. The data show that the increase in BChl *c* antenna of *Osc. trichoides* chlorosomes by ~ 1.6 -fold controlled by light intensity during cell culture growth is accompanied by the increase in hyperchromism of BChl *c* absorption Q_y band by $\sim 9\%$. For *Cfx. aurantiacus* chlorosomes, the same increase in chlorosomal BChl *c* antenna corresponds to hyperchromism increase by 10% (Tables 2 and 3). This means that the dependence of $H(\eta)$ for *Cfx. aurantiacus* chlorosomes and similar dependence for *Osc. trichoides* are phenomenologically identical.

Thus, the measured dependences $H(\eta)$ in *Cfx. aurantiacus* and *Osc. trichoides* chlorosomes have essentially the same character, indicating that:

- the size (*n*) of the unit BChl *c* oligomer of both *Osc. trichoides* and *Cfx. aurantiacus* chlorosomes corresponds to the limit of the small aggregate of bacterial antenna ($n \approx 5$);
- increase in size of the entire chlorosomal antenna of *Osc. trichoides* as well as that of *Cfx. aurantiacus* leads to increase in size of its unit BChl *c* oligomer.

It is necessary to note that the conclusions of our works do not depend on which model of three-dimensional chlorosome structures (tubular or lamellar) is realized *in vivo*, because the degree of pigment aggregation can be the variable factor in either model. Namely, this structural factor is the determining factor for high efficiency of functioning of such variable size antennas [11].

Table 3. Relative value of hyperchromism (H) of absorption Q_y band for BChl *c* from *Osc. trichoides* chlorosomes C-70 and C-110

<i>Osc. trichoides</i> chlorosomes	H, relative units
C-70	1.0
C-110	1.09

Note: The chlorosome C-70 hyperchromism value was taken as 1.0.

We suggest that our proposed strategy of effective functioning of peripheral oligomeric antennas, namely, culture growth light intensity-controlled variability of the degree of aggregation of the unit building block of peripheral antenna, is the universal strategy for photosynthesizing organisms.

To date, such a strategy has been revealed not only for green bacteria, but also for the purple photosynthetic bacterium *Rhodospseudomonas palustris*. A structure of new peripheral BChl *a* antenna complex B 800 LH-2 adapted to weak light was shown in work [42] by Hartigan et al. with the use of X-ray crystallography. It was shown that with light intensity decrease during *Rh. palustris* growth, the unit building block of peripheral BChl *a* antenna complex B 800-850 LH-2 (composed of one monomer B 800 and one dimer B 850) increased in size with formation of a new aggregate of four exciton-coupled BChl *a* molecules, i.e. actually it was shown the growth light intensity-controlled variability of the degree of aggregation of the unit building block of peripheral antenna when the entire antenna size changed.

Thus, we conclude that light controls not only the size of the peripheral oligomeric BChl *c* antenna, but also the size of its unit building block, allowing green photosynthetic bacteria to survive over a wide range of light intensities. Under lower growth light intensity the BChl *c* antenna size increases, thus compensating light deficiency by increasing the light-absorbing capability of the antenna. An inevitable drop in the efficiency of the antenna functioning with increasing its size [1], in turn, is compensated by an increase in the size of the unit BChl *c* building block of the oligomeric antenna, thus ensuring high efficiency of functioning of the antenna regardless of its size.

This work was partly supported by the Russian Foundation for Basic Research (grants 10-04-01758a and 11-04-00312a).

REFERENCES

- Fetisova, Z. G., and Fok, M. V. (1984) *Mol. Biol. (Moscow)*, **18**, 1651-1656.
- Fetisova, Z. G., Fok, M. V., and Shibaeva, L. V. (1985) *Mol. Biol. (Moscow)*, **19**, 983-991.
- Timpmann, K. E., Freiberg, A. M., and Fetisova, Z. G. (1988) *Dokl. Akad. Nauk SSSR*, **302**, 976-979.
- Fetisova, Z. G., Freiberg, A. M., and Timpmann, K. E. (1988) *Nature*, **334**, 633-634.
- Fetisova, Z. G., Shibaeva, L. V., and Fok, M. V. (1989) *J. Theor. Biol.*, **140**, 167-184.
- Fetisova, Z. G., and Muring, K. (1992) *FEBS Lett.*, **307**, 371-374.
- Fetisova, Z. G., Muring, K., and Taisova, A. S. (1994) *Photosynth. Res.*, **41**, 205-210.
- Fetisova, Z. G., Shibaeva, L. V., and Taisova, A. S. (1995) *Mol. Biol. (Moscow)*, **29**, 1384-1390.
- Muring, K., Taisova, A. S., Novoderezhkin, V. I., Shibaeva, L. V., and Fetisova, Z. G. (1996) *Mol. Biol. (Moscow)*, **30**, 442-448.
- Krasnovsky, A. A., and Bystrova, M. I. (1980) *Biosystems*, **12**, 181-194.
- Fetisova, Z. G. (2004) *Mol. Biol. (Moscow)*, **38**, 515-523.
- Yakovlev, A. G., Taisova, A. S., and Fetisova, Z. G. (2004) *Mol. Biol. (Moscow)*, **38**, 524-531.
- Keppen, O. I., Tourova, T. P., Kuznetsov, B. B., Ivanovsky, R. N., and Gorlenko, V. M. (2000) *Int. J. System. Evol. Microbiol.*, **50**, 1529-1537.
- Taisova, A. S., Keppen, O. I., Lukashev, E. P., Arutyunyan, A. M., and Fetisova, Z. G. (2002) *Photosynth. Res.*, **74**, 73-85.
- Gupta, R. S., Chander, P., and George, S. (2013) *Antonie van Leeuwenhoek*, **103**, 99-119.
- Orf, G. S., and Blankenship, R. E. (2013) *Photosynth. Res.*, **116**, 315-331.
- Oostergetel, G. T., van Amerongen, H., and Boekema, E. J. (2010) *Photosynth. Res.*, **104**, 245-255.
- Staelin, L. A., Golecki, J. R., Fuller, R. C., and Drews, G. (1978) *Arch. Microbiol.*, **119**, 269-277.
- Staelin, L. A., Golecki, J. R., and Drews, G. (1980) *Biochim. Biophys. Acta*, **589**, 30-45.
- Psencik, J., Ikonen, T. P., Laurinmaki, P., Merckel, M. C., Butcher, S. J., Serimaa, R. E., and Tuma, R. (2004) *Biophys. J.*, **87**, 1165-1172.
- Linnanto, J. M., and Korppi-Tommola, J. E. I. (2013) *J. Phys. Chem. B*, **117**, 11144-11161.
- Fetisova, Z. G., Freiberg, A. M., Muring, K., Novoderezhkin, V. I., Taisova, A. S., and Timpmann, K. E. (1996) *Biophys. J.*, **71**, 995-1010.
- Novoderezhkin, V. I., and Fetisova, Z. G. (1996) *Biochem. Mol. Biol. Int.*, **40**, 243-252.
- Dracheva, T. V., Taisova, A. S., and Fetisova, Z. G. (1998 in *Photosynthesis: Mechanisms and Effects*, Vol. 1 (Garab, G., ed.) Kluwer Academic Publishers, The Netherlands, pp. 129-132.
- Novoderezhkin, V. I., Taisova, A. S., and Fetisova, Z. G. (2001) *Chem. Phys. Lett.*, **335**, 234-240.
- Yakovlev, A. G., Novoderezhkin, V. I., Taisova, A. S., and Fetisova, Z. G. (2002) *Photosynth. Res.*, **71**, 19-32.
- Pierson, B. K., and Castenholz, R. W. (1974) *Arch. Microbiol.*, **100**, 283-305.
- Taisova, A. S., Keppen, O. I., and Fetisova, Z. G. (2004) *Biofizika (Moscow)*, **49**, 1069-1074.
- Feick, R. G., Fitzpatrick, M., and Fuller, R. C. (1982) *J. Bacteriol.*, **150**, 905-915.
- Van Dorssen, R. J., Vasmel, H., and Ames, J. (1986) *Photosynth. Res.*, **9**, 33-45.
- Mukamel, S. (1995) *Principles of Nonlinear Optical Spectroscopy*, Oxford University Press, New York-Oxford.
- Novoderezhkin, V., Monshouwer, R., and van Grondelle, R. (1999) *J. Phys. Chem. B*, **103**, 10540-10548.
- Savikhin, S., Buck, D. R., Struve, W. S., Blankenship, R. E., Taisova, A. S., Novoderezhkin, V. I., and Fetisova, Z. G. (1998) *FEBS Lett.*, **430**, 323-326.
- Meier, T., Chernyak, V., and Mukamel, S. (1997) *J. Phys. Chem. B*, **101**, 7332-7342.
- Nagarajan, V., Johnson, E. T., Williams, J. C., and Parson, W. W. (1999) *J. Phys. Chem. B*, **103**, 2297-2309.

36. Pullerits, T., Chachisvilis, M., and Sundstrom, V. (1996) *J. Phys. Chem. B*, **100**, 10787-10792.
37. Novoderezhkin, V. I., and Fetisova, Z. G. (1999) *Biophys. J.*, **77**, 424-430.
38. Keppen, O. I. (2010) in *Works of S. N. Vinogradsky Institute of Microbiology*, Issue 15. *Photosynthesizing Microorganisms* (Galchenko, V. F., ed.) [in Russian], Maks Press, Moscow, pp. 196-222.
39. Taisova, A. S., Gülen, D., Iseri, E. I., Drachev, V. A., Cherenkova, T. A., and Fetisova, Z. G. (2001) *Thesis of XII Int. Congr. on Photosynthesis* (Brisbane, Australia), Abstr. S1-006.
40. Yildirim, H., Iseri, I., and Gülen, D. (2004) *Chem. Phys. Lett.*, **391**, 302-307.
41. Gülen, D. (2006) *Photosynth. Res.*, **87**, 205-214.
42. Hartigan, N., Tharia, H. A., Sweeney, F., Lawless, A. M., and Papiz, M. Z. (2002) *Biophys. J.*, **82**, 963-977.